

Low temperature Correlation lengths of Bilayer Heisenberg Antiferromagnets and Neutron Scattering

Lan Yin and Sudip Chakravarty

Department of Physics and Astronomy, University of California, Los Angeles, CA 90095

(February 1, 2008)

Abstract

The low temperature correlation length and the static structure factor are computed for bilayer antiferromagnets such as $\text{YBa}_2\text{Cu}_3\text{O}_6$. It is shown that energy integrated two-axis scan in neutron scattering experiments can be meaningfully interpreted to extract correlation length in such bilayer antiferromagnets despite intensity modulation in the momentum perpendicular to the layers. Thus, precise measurements of the spin-spin correlation length can be performed in the future, and the theoretical predictions can be tested. It is also shown how the same correlation length can be measured in nuclear magnetic resonance experiments.

PACS: 75.10.Jm, 74.72.Bk

Nearly thirty five years ago Birgeneau, Skalyo and Shirane [1] invented a neutron scattering method, known as the energy integrated two-axis scan (ETAS), whereby the spin-spin correlation lengths of layered magnets can be measured without explicitly measuring the dynamic structure factor for all energy and momentum transfers and then integrating over the energy, known as the three axis scan. Except for special circumstances, three axis scan to measure correlation length is difficult.

The underlying principles of ETAS are an analog energy integration performed by using a special geometry and the reliance on the dominance of low energy scattering—the method is especially effective when the critical scattering dominates. In recent years, ETAS has served us well in unravelling the magnetic fluctuations of the parent compound of one of the high temperature superconductors, namely the La_2CuO_4 [2]. The experimental results are in excellent agreement with our theoretical understanding of these two-dimensional magnets [3]. Unfortunately, the method does not appear to be readily extendable to a wide class of high temperature superconductors with close magnetic bilayers or triple layers within the unit cell; a particularly important example is $\text{YBa}_2\text{Cu}_3\text{O}_6$, which has a close pair of magnetic planes within the unit cell, but it is otherwise a square lattice spin $S = 1/2$ Heisenberg antiferromagnet. The reason for the difficulty of using ETAS is an intensity modulation [4] with the momentum transfer perpendicular to the planes.

It is the purpose of the present paper to (a) derive the low temperature properties of such bilayer antiferromagnets and (b) to show how ETAS can be extended to such bilayer antiferromagnets. It is hoped that future experiments using ETAS will be able to provide us with precise measurements of the antiferromagnetic correlation lengths in these materials, which should be of great help in understanding the magnetic fluctuations of these bilayer superconductors. We also briefly remark how the same correlation length can be also measured by measuring the Cu relaxation rate in nuclear magnetic resonance (NMR) experiments.

The Heisenberg model for a spin- S , nearest neighbor, square lattice, bilayer antiferromagnet is

$$H = J_{\parallel} \sum_{\langle ij \rangle, p} \mathbf{S}_i^{(p)} \cdot \mathbf{S}_j^{(p)} + J_{\perp} \sum_i \mathbf{S}_i^{(1)} \cdot \mathbf{S}_i^{(2)}. \quad (1)$$

The sum in the first term is over the nearest neighbor pairs in each plane, where the plane index p takes two values 1 and 2. The second term represents the coupling between the planes. The exchange constants J_{\parallel} and J_{\perp} are both positive.

The low energy, long wavelength properties of the two dimensional Heisenberg model is well described by the quantum $O(3)$ nonlinear σ -model [5]. Here, we shall consider its generalization to coupled bilayers. The Euclidean action for this system can be written down on general symmetry grounds [5], but it can also be derived from a $(1/S)$ expansion [6]. The action is

$$S = \int_0^u dx_0 \int d^2x \left[\sum_{p=1}^2 \left(\frac{1}{2g_0} |\partial_{\mu} \hat{\Omega}^{(p)}|^2 - h_0 \sigma^{(i)} \right) + \frac{1}{2g_{\perp}^0} |\hat{\Omega}^{(1)} - \hat{\Omega}^{(2)}|^2 - \frac{1}{2g_t^0} (\hat{\Omega}^{(1)} \times \partial_0 \hat{\Omega}^{(1)}) \cdot (\hat{\Omega}^{(2)} \times \partial_0 \hat{\Omega}^{(2)}) \right], \quad (2)$$

where $\sigma^{(p)}$ is the component of the staggered field $\hat{\Omega}^{(p)}$ in the direction of the staggered magnetic field h . Here, all the coupling constants and dimensional variables have been scaled to their dimensionless forms. The label $\mu = 1, 2$ denotes the spatial directions, and $\mu = 0$ corresponds to the imaginary time direction. The extent in the imaginary time direction is given by u , where c_0 is the spin-wave velocity. For mathematical purposes, it is possible to extend the action to dimensions, d , other than 2 and to the general symmetry group $O(N)$. It is only for $d = 2$ and $N = 3$, however, that the model represents a bilayer antiferromagnet. Since there are no difficulties in working directly with $d = 2$ and $N = 3$, we shall use these parameters throughout the paper. For later convenience, we define $\tilde{h}_0 = h_0 g_0$, $\tilde{\gamma}_{\perp}^0 = \frac{2g_0}{g_{\perp}^0}$, and $\tilde{\delta}_t^0 = \frac{g_0}{2g_t^0}$.

The relations between the σ -model parameters and the Heisenberg model parameters are known in the large- S limit [6]. After correcting minor errors, the correct relations, in the limit $S \rightarrow \infty$, are $g_0 = \frac{\hbar c_0 \sqrt{1-\tilde{\delta}_t^0} \Lambda}{\rho_s^0}$, $g_{\perp}^0 = \frac{\hbar c_0 \sqrt{1-\tilde{\delta}_t^0} \Lambda (\Lambda a)^2}{\rho_{\perp}^0}$, $g_t^0 = \frac{4\hbar c_0 \Lambda}{\rho_{\perp}^0 \sqrt{1-\tilde{\delta}_t^0}}$, and $u = \beta \hbar c_0 \sqrt{1-\tilde{\delta}_t^0} \Lambda$, where $\tilde{\delta}_t^0 = \frac{J_{\perp}}{8J_{\parallel}+J_{\perp}}$; the spin-stiffness constants are $\rho_s^0 = J_{\parallel} S^2$ and $\rho_{\perp}^0 = J_{\perp} S^2$, and the spin wave velocity is $c_0 = \frac{aS}{\hbar} \sqrt{2J_{\parallel}(4J_{\parallel}+J_{\perp})}$. The quantity a is the lattice constant of the

Heisenberg model, and the momentum cutoff is given by $\Lambda = \frac{\sqrt{2\pi}}{a}$ to conserve the number of degrees of freedom.

Our calculations show explicitly [7] that the angular momentum coupling between the layers is irrelevant for weakly coupled bilayer systems such as $\text{YBa}_2\text{Cu}_3\text{O}_6$, although it breaks the ‘‘Lorentz invariance’’ and renormalizes the spin-wave velocity. The angular momentum coupling term also reduces to a higher gradient term when the number of layers tends to infinity. We shall omit this term from our further discussion.

This bilayer model has a massless mode and a massive mode. We can see this by simply expanding the action to quadratic order:

$$S_2 = \int_0^u dx_0 \int d^2x \frac{1}{4g_0} \left[|\partial_\mu(\boldsymbol{\pi}^{(1)} + \boldsymbol{\pi}^{(2)})|^2 + \tilde{h}_0 |\boldsymbol{\pi}^{(1)} + \boldsymbol{\pi}^{(2)}|^2 + |\partial_\mu(\boldsymbol{\pi}^{(1)} - \boldsymbol{\pi}^{(2)})|^2 + (\tilde{h}_0 + \tilde{\gamma}_\perp^0) |\boldsymbol{\pi}^{(1)} - \boldsymbol{\pi}^{(2)}|^2 \right], \quad (3)$$

where $\boldsymbol{\pi}^{(i)}$ is the transverse component of $\hat{\boldsymbol{\Omega}}^{(i)}$. In the absence of staggered field $\tilde{h}_0 = 0$, the symmetric combination is gapless, and the antisymmetric combination has a gap $\sqrt{\tilde{\gamma}_\perp^0}$, which will be called the bare dimensionless bilayer gap; the bare dimensional bilayer gap is given by $\hbar c_0 \Lambda \sqrt{\tilde{\gamma}_\perp^0}$. At finite temperatures, the massless mode becomes massive due to interactions, which is a topic of this paper.

We carry out one-loop momentum-shell calculations similar to those of Ref. [5] and obtain the following renormalization group equations

$$\frac{dg}{dl} = -g + \frac{g^2}{8\pi} \left[\frac{\coth(\frac{g}{2t}\sqrt{1+\tilde{h}})}{\sqrt{1+\tilde{h}}} + \frac{\coth(\frac{g}{2t}\sqrt{1+\tilde{h}+\tilde{\gamma}_\perp})}{\sqrt{1+\tilde{h}+\tilde{\gamma}_\perp}} \right], \quad (4)$$

$$\frac{dt}{dl} = \frac{gt}{8\pi} \left[\frac{\coth(\frac{g}{2t}\sqrt{1+\tilde{h}})}{\sqrt{1+\tilde{h}}} + \frac{\coth(\frac{g}{2t}\sqrt{1+\tilde{h}+\tilde{\gamma}_\perp})}{\sqrt{1+\tilde{h}+\tilde{\gamma}_\perp}} \right], \quad (5)$$

$$\frac{d\tilde{h}}{dl} = 2\tilde{h}, \quad (6)$$

$$\frac{d\tilde{\gamma}_\perp}{dl} = 2\tilde{\gamma}_\perp - \frac{g\tilde{\gamma}_\perp}{4\pi} \frac{\coth(\frac{g}{2t}\sqrt{1+\tilde{h}+\tilde{\gamma}_\perp})}{\sqrt{1+\tilde{h}+\tilde{\gamma}_\perp}}, \quad (7)$$

where e^l is the length rescaling factor. The variable t is the dimensionless temperature

variable. The dimensionless thickness of the slab in the imaginary time direction $u = g/t$ satisfies a simple scaling relation given by $(g/t) = (g_0/t_0)e^{-l}$.

The zero temperature flows of the renormalization group equations are shown in Fig.1. There are two phases, separated by a separatrix between the two unstable fixed points $(g = 4\pi, g_\perp = \infty)$ and $(g = 8\pi, g_\perp = 0)$; the former is the fixed point of the single layer case [5]. There are two stable fixed points. The ordered-phase fixed point is located at $(0, 0)$, where both the in- and the inter-plane couplings are infinitely strong. The disordered-phase fixed point is located at (∞, ∞) , where the system becomes totally disordered. Although quantum nonlinear σ -model is a very accurate description of the low energy physics in or near the ordered phase [5], far into the disordered phase, such a continuum theory can not be expected to be valid.

In the bilayer, $S = 1/2$ Heisenberg model, a quantum phase transition takes place when $J_\perp \geq 2.55J_\parallel$ [10]. In the σ -model, the phase transition takes place at a critical value of g for any g_\perp . At present, we do not have an accurate mapping between the Heisenberg model parameters and the σ -model parameters allowing us to relate the quantum disordered phases of these two models. In the quantum disordered phase, the large- S analysis is not appropriate because it relies on the existence of goldstone modes that are not present in this phase.

The parameters applicable to $\text{YBa}_2\text{Cu}_3\text{O}_{6+x}$ lie in the ordered phase, where $\tilde{\gamma}_\perp^0 \sim \frac{J_\perp}{J_\parallel} \ll 1$, and g is below the critical value required for the phase transition to the quantum disordered phase at $T = 0$. Therefore, the system is in the renormalized classical regime [5]. Also, from experiments, it is known that the ground state is an ordered Néel state and that $J_\perp \sim 0.1J_\parallel$ [9].

To proceed further, we need an analytical solution of the renormalization group equations. We have obtained a good approximation to the solution based on the following observations. In the renormalized classical regime, the bilayer gap $\sqrt{\tilde{\gamma}_\perp}$ is initially much smaller than unity, but increases as $\sqrt{\tilde{\gamma}_\perp} \propto e^{\alpha(l)l/2}$, where $\alpha(l) < 2$, but tends to 2 for large l . We can therefore consider two regions, $\tilde{\gamma}_\perp \ll 1$ in region (I), and $\frac{d\tilde{\gamma}_\perp}{dl} \simeq 2\tilde{\gamma}_\perp$ in the region (II). We solve the renormalization group equations separately in regions (I) and (II), and then

join the two solutions together to get the final answer. In (I), we replace $\sqrt{1 + \tilde{\gamma}_\perp}$ by unity and obtain

$$\frac{1}{t_0} - \frac{1}{t_1} = \frac{1}{2\pi} \left[\ln \sinh\left(\frac{g_0}{2t_0}\right) - \ln \sinh\left(\frac{g_0}{2t_0} e^{-l_1}\right) \right], \quad (8)$$

$$\tilde{\gamma}_\perp^1 = \frac{t_0}{t_1} \tilde{\gamma}_\perp^0 e^{2l_1}, \quad (9)$$

where $(l_1, t_1, \tilde{\gamma}_\perp^1)$ are the variables at the endpoint of (I). In (II), we use $\frac{d\tilde{\gamma}_\perp}{dl} = 2\tilde{\gamma}_\perp$ and get

$$\frac{1}{t_1} - \frac{1}{t} = \frac{1}{4\pi} \ln \left[\frac{\sinh\left(\frac{g_0}{2t_0} e^{-l_1}\right) \sinh\left(\frac{g_0}{2t_0} e^{-l_1} \sqrt{1 + \tilde{\gamma}_\perp^1}\right)}{\sinh\left(\frac{g_0}{2t_0} e^{-l}\right) \sinh\left(\frac{g_0}{2t_0} e^{-l_1} \sqrt{e^{-2(l-l_1)} + \tilde{\gamma}_\perp^1}\right)} \right]. \quad (10)$$

The initial condition $\tilde{\gamma}_\perp^0 \ll 1$ guarantees that the crossover between (I) and (II) is smooth, namely, $\tilde{\gamma}_\perp^1 \ll 1$ and $\frac{d\tilde{\gamma}_\perp}{dl}|_{l_1} \simeq 2\tilde{\gamma}_\perp^1$. Since we can choose l_1 such that $\tilde{\gamma}_\perp^0 \ll e^{-2l_1} \ll 1$, this guarantees that $\tilde{\gamma}_\perp^1 \ll 1$ from Eq. (9). The initial temperature is low enough that both $\frac{g_0}{2t_0}$ and $\frac{g_0}{2t_0} e^{-l_1}$ are much larger than unity. Following Eq. (8), we get $\frac{1}{t_1} \simeq \frac{1}{t_0} (1 - \frac{g_0}{4\pi})$. At this point, the second term in Eq. (7) becomes negligible because $\frac{g}{4\pi} \frac{\coth(\frac{g}{2t} \sqrt{1 + \tilde{\gamma}_\perp})}{\sqrt{1 + \tilde{\gamma}_\perp}} \simeq \frac{g_0 t_1}{4\pi t_0} e^{-l_1} = \frac{g_0}{4\pi - g_0} e^{-l_1} \ll 2$; therefore $\frac{d\tilde{\gamma}_\perp}{dl}|_{l_1} \simeq 2\tilde{\gamma}_\perp^1$ is also true.

The two solutions can now be combined together to get

$$\frac{1}{t_0} - \frac{1}{t} = \frac{1}{4\pi} \ln \left[\frac{\sinh^2\left(\frac{g_0}{2t_0}\right)}{\sinh\left(\frac{g_0}{2t_0} e^{-l}\right) \sinh\left(\frac{g_0}{2t_0} \sqrt{e^{-2l} + e^{-2l_1} \tilde{\gamma}_\perp^1}\right)} \right]. \quad (11)$$

The single layer result

$$\frac{1}{t_0} - \frac{1}{t} = \frac{1}{2\pi} \left[\ln \sinh\left(\frac{g_0}{2t_0}\right) - \ln \sinh\left(\frac{g_0 e^{-l}}{2t_0}\right) \right] \quad (12)$$

is trivially recovered when the bilayer gap is much smaller than the inverse correlation length, that is, $\sqrt{\tilde{\gamma}_\perp^0} \ll e^{-l}$.

In the limit of large l , the solution has the asymptotic form of $\frac{2}{t} = \frac{2}{t_{\text{eff}}} - \frac{l}{2\pi}$, where

$$\frac{1}{t_{\text{eff}}} = \frac{1}{t_0} \left(1 - \frac{g_0}{4\pi}\right) + \frac{1}{4\pi} \ln \left[\frac{2g_0}{t_0} \sinh\left(\frac{g_0}{2t_0} \sqrt{\tilde{\gamma}_\perp^0 \left(1 - \frac{g_0}{4\pi}\right)}\right) \right]. \quad (13)$$

This is identical to the low temperature limit of the solution of a classical single-layer σ -model: $\frac{1}{t^{\text{cl}}} = \frac{1}{t_0^{\text{cl}}} - \frac{l}{2\pi}$. Thus, we can map the quantum bilayer model to the classical single

layer model by identifying $\frac{2}{t_{\text{eff}}} = \frac{1}{t_0^{\text{cl}}}$ and $\frac{2}{t} = \frac{1}{t^{\text{cl}}}$. The remaining arguments as to how to combine the classical two-loop result, along with the conversion of the prefactor from the continuum to the lattice, are the same as those given in Ref. [5]. We get

$$\xi = \frac{e}{8} \Lambda^{-1} \frac{t_{\text{eff}}}{4\pi} e^{\frac{4\pi}{t_{\text{eff}}}}, \quad (14)$$

with the exact prefactor determined in Ref. [8].

An important result is that the argument of the exponential is twice of that of the single layer case. This factor of 2 comes from the mapping between the bilayer model and the single layer model. To get a feeling for this factor, it is instructive to consider a classical bilayer model given by the action $S = \frac{1}{t^{\text{cl}}} \int d^2x \left[\sum_{i=1}^2 \left(|\partial_\mu \hat{\Omega}^{(i)}|^2 - \tilde{h} \sigma^{(i)} \right) + \frac{\tilde{\gamma}_\perp}{2} \left| \hat{\Omega}^{(1)} - \hat{\Omega}^{(2)} \right|^2 \right]$. To map it on to the single layer model, we need to define a new field $\hat{\Omega}$, where the transverse components are given by $\boldsymbol{\pi} = \frac{1}{2}(\boldsymbol{\pi}^{(1)} + \boldsymbol{\pi}^{(2)})$, and the longitudinal component is given by $\sigma = \sqrt{1 - |\boldsymbol{\pi}|^2}$. This can be accomplished by integrating out the massive fields $\frac{1}{2}(\boldsymbol{\pi}^{(1)} - \boldsymbol{\pi}^{(2)})$. The result is the new action $S' = \frac{2}{t^{\text{cl}}} \int d^2x \left(|\partial_\mu \hat{\Omega}|^2 - h\sigma \right)$, consistent with our previous result.

When temperature is low enough such that $\frac{g_0}{2t_0} \sqrt{\tilde{\gamma}_\perp^0} > 1$, the correlation length can be written as

$$\xi = \frac{e}{8} \frac{\hbar c}{4\pi \rho_s(0)} e^{\frac{4\pi \rho_s(0)}{k_B T}}, \quad (15)$$

where $\rho_s(0)$ is the renormalized spin stiffness constant, which within one-loop approximation is given by $\rho_s(0) = \rho_s^0 \left[1 - \frac{g_0}{4\pi} \left(1 - \frac{1}{2} \sqrt{\tilde{\gamma}_\perp^0 (1 - \frac{g_0}{4\pi})} \right) \right]$. As discussed in Ref. [5], the formula can be used with $\rho_s(0)$ the exact spin stiffness constant of the bilayer Heisenberg model.

The numerical value of the spin stiffness constant can be obtained from spin-wave theory, and it is given by $\rho_s(0) = J_\parallel S^2 Z_c(S) Z_\chi(S)$. For $S = (1/2)$, $J_\perp = 0.08J_\parallel$ [9], and up to order of $(1/S)$, we get $Z_c(S) = 1.153$, $Z_\chi(S) = 0.531$, and $\rho_s(0) = 0.176J_\parallel$. Therefore the correlation length is given by

$$\xi \simeq 0.25ae^{\frac{4\pi \rho_s(0)}{k_B T}}, \quad (16)$$

where a is the lattice spacing. The exponential temperature dependence is identical to the single layer case, but the factor of 2 in the exponent should be noted.

The static structure factor can be obtained in the same way as in Ref. [5]. For the bilayer case, it contains two pieces, one for the symmetric combination of the unit vectors from each layer and the other for the antisymmetric combination. The notation in the σ -model is exactly the opposite to the notation in the Heisenberg model, since the unit vector field $\hat{\Omega}^{(p)}$ in the σ -model is the continuum limit of the direction vector of the staggered spin operator $(-1)^{i+p}\mathbf{S}_i^{(p)}$ in the Heisenberg model. Our renormalization group equations show that in the long wavelength limit both pieces satisfy the following equation as in the single layer case [5]

$$S(k, t_0) = e^{2l} \left(\frac{t_0}{t}\right)^2 S(e^l k, t), \quad (17)$$

where $t \equiv t(l)$ is the running coupling constant and k is defined with respect to the antiferromagnetic wavevector $(\pi/a, \pi/a)$.

For the symmetric piece, we evaluate the right hand side at $l = l^*$ such that we are far into the disordered regime, either because the correlation length is of order unity or because the rescaled wave vector ke^l is sufficiently large. These requirements are satisfied by choosing a l^* such that $\xi^{-2}(t_0)e^{2l^*} + k^2e^{2l^*} = 1$. When this condition is satisfied, we can approximate $S_s[e^{l^*}k, t(l^*)]$ by the Ornstein-Zernicke form

$$S_s[e^{l^*}k, t(l^*)] \simeq \frac{t(l^*)}{\xi^{-2}(l^*) + k^2(l^*)}. \quad (18)$$

Then,

$$S_s(k, t_0) = \frac{t_0^2 \xi^2}{2\pi} f(x), \quad (19)$$

where $x = k\xi$ and $f(x) = \frac{1+\frac{1}{2}\ln(1+x^2)}{1+x^2}$.

The antisymmetric piece can be obtained in a similar manner. When $l \simeq l^*$, the bilayer gap $\sqrt{\tilde{\gamma}_\perp}$ is increased by a factor e^{l^*} . At this point, it is safe to assume the Ornstein-Zernicke form

$$S_a(e^{l^*}k, t(l^*)) \simeq \frac{2t(l^*)}{e^{2l^*}(\xi_\perp^{-2} + k^2)}, \quad (20)$$

where ξ_\perp is the length scale associated with the bilayer gap. Approximately, we have $\xi_\perp \simeq e^{-l^*} \sqrt{\tilde{\gamma}_\perp}/\Lambda \simeq \sqrt{(1 - \frac{g_0}{4\pi})\tilde{\gamma}_\perp^0}/\Lambda$. In terms of the initial coupling constants, we get

$$S_a(k, t_0) \simeq \frac{(2 - \frac{g_0}{2\pi})t_0}{k^2 + \xi_\perp^{-2}}. \quad (21)$$

The symmetric piece is dominant in the long-wavelength limit because

$$\frac{S_s(0, t_0)}{S_a(0, t_0)} \sim t_0 \frac{\xi^2}{\xi_\perp^2} \gg 1. \quad (22)$$

In ETAS, the wavevector of the incoming neutron \mathbf{q}_i is fixed, while the outgoing neutrons in a direction perpendicular to the layers are collected, regardless of their energies. The transferred wavevector is given by $\mathbf{q} = \mathbf{q}_f - \mathbf{q}_i$. Its in-plane component \mathbf{q}_{\parallel} is a constant, $\mathbf{q}_{\parallel} = -\mathbf{q}_{i\parallel}$, while its perpendicular component is a variable, $q_\perp = q_f - q_{i\perp}$. For \mathbf{q}_{\parallel} near reciprocal lattice vectors, the form factor is approximately a constant, and the intensity $I(\mathbf{q}_{\parallel})$ is proportional to $\int_0^\infty dq_f S^{3D}(\mathbf{q}, \frac{\hbar^2}{2m}(q_f^2 - q_i^2))$, where $S^{3D}(\mathbf{q}, \omega)$ is the 3D dynamic structure factor. It is related to the 2D dynamic structure factors by $S^{3D}(\mathbf{q}, \omega) = \sin^2(\frac{q_\perp h}{2})S_a^{2D}(\mathbf{q}_{\parallel}, \omega) + \cos^2(\frac{q_\perp h}{2})S_s^{2D}(\mathbf{q}_{\parallel}, \omega)$, where h is the distance between the two layers. The quantity $S_a^{2D}(\mathbf{q}_{\parallel}, \omega)$ corresponds to the antisymmetric spin combination with respect to the layers, *symmetric* in the σ -model sense, and $S_s^{2D}(\mathbf{q}_{\parallel}, \omega)$ to the corresponding symmetric spin combination, *antisymmetric* in the σ -model sense. In experiments one probes the region $\mathbf{q}_{\parallel} \approx \mathbf{G}$, where \mathbf{G} is the nearest antiferromagnetic reciprocal lattice vector. Defining $\mathbf{k} = \mathbf{q}_{\parallel} - \mathbf{G}$, we can rewrite the intensity in terms of the σ -mode

structure factors, recalling that the definitions of the symmetric and the antisymmetric combinations get switched in going from the spin picture to the σ -model picture. The intensity contains two pieces, $I(\mathbf{k}) = I_s(\mathbf{k}) + I_a(\mathbf{k})$, where

$$I_s(\mathbf{k}) \sim \int_0^\infty dq_f \sin^2 \frac{(q_f - q_{i\perp})h}{2} S_s^{2D\sigma}(\mathbf{k}, \frac{\hbar^2}{2m}(q_f^2 - q_i^2)), \quad (23)$$

$$I_a(\mathbf{k}) \sim \int_0^\infty dq_f \cos^2 \frac{(q_f - q_{i\perp})h}{2} S_a^{2D\sigma}(\mathbf{k}, \frac{\hbar^2}{2m}(q_f^2 - q_i^2)). \quad (24)$$

The q_\perp -modulation is unimportant in the critical region. The reason is that $S_s^{2D\sigma}(\mathbf{k}, \omega)$ is dominated by the critical fluctuations near $\omega = 0$, where both $\sin^2\left(\frac{(q_f - q_{i\perp})h}{2}\right)$ and

$\frac{d\omega}{dq_f} = \frac{\hbar^2}{m} q_f$ are essentially constants. Therefore, we can pull these factors out of the integral and obtain the intensity approximately proportional to the static structure factor, $I_s(\mathbf{k}) \sim \frac{m}{\hbar^2 q_i} \sin^2\left(\frac{(q_i - q_{i\perp})}{2} h\right) \int_{-E_i}^{\infty} d\omega S_s^{2D\sigma}(\mathbf{k}, \omega) \sim S_s(\mathbf{k}, t_0)$, where we have reverted to the previous notation by dropping the superscripts. The quantity E_i is the incident neutron energy. For the antisymmetric piece, we get an upper bound by neglecting the factor $\cos^2(\frac{q_{i\perp} h}{2})$, which is $\int_0^{\infty} dq_f S_a^{2D\sigma}(\mathbf{k}, \frac{\hbar^2}{2m}(q_f^2 - q_i^2)) \sim \frac{m}{\hbar^2 \langle q_f \rangle} S_a(\mathbf{k}, t_0)$, where $\langle q_f \rangle$ is some average of the wavevector. Because $S_s(0, t_0) \gg S_a(0, t_0)$, the intensity is dominated by the contribution from the symmetric piece. Therefore ETAS for a bilayer should yield information about the symmetric piece, hence the correlation length. The contribution of the antisymmetric piece should result in a small broad background.

The NMR relaxation rate for the in-plane Cu site will be given by [11] $\frac{1}{T_1} \propto T^{\frac{3}{2}} \xi$, because the symmetric structure factor will dominate when the correlation length ξ is large. Thus, the formula for the correlation length, Eq. (15), can also be tested in NMR experiments, as for the single layer La_2CuO_4 [12].

In conclusion, we have computed the low temperature properties of bilayer antiferromagnets using a quantum nonlinear σ -model approach. Explicit results were given for the static structure factor and the correlation length. The correlation length diverges exponentially as $T \rightarrow 0$, but the striking feature is that the argument of the exponential function is a factor of 2 larger than the corresponding single layer case. We have also shown that ETAS and NMR can be used to test our theoretical predictions concerning the correlation length.

We thank O. Syljuåsen for discussions. This work was supported by the National Science Foundation, Grant. No. DMR-9531575.

REFERENCES

- [1] R. J. Birgeneau, J. Skalyo and G. Shirane, Phys. Rev. B **3**, 1736 (1971)
- [2] Y. Endoh *et al.*, Phys. Rev. B **37**, 7443 (1988); K. Yamada *et al.*, Phys. Rev. B **40**, 4557 (1989).
- [3] For a theoretical review, see S. Chakravarty in *High temperature superconductivity*, edited by K. S. Bedell *et al.* (Addison-Wesley, Redwood City, 1990). For an experimental review, see M. Greven *et al.*, Z. Phys. B **96**, 465 (1995).
- [4] S. Shamoto *et al.*, Phys. Rev. B **48**, 13817 (1993)
- [5] S. Chakravarty, B. I. Halperin, and D. R. Nelson, Phys. Rev. B **39**, 2344 (1989).
- [6] A. V. Dotsenko, Phys. Rev. B **52**, 9170 (1995)
- [7] The renormalization group equation for the angular momentum coupling is given by $d\tilde{\delta}_t/dl = -(\tilde{\delta}_t g/4\pi) \left[\coth \left(\frac{g}{2t} \sqrt{\frac{1+\tilde{h}+\tilde{\gamma}_\perp}{1+\tilde{\delta}_t}} \right) / \sqrt{(1+\tilde{h}+\tilde{\gamma}_\perp)(1+\tilde{\delta}_t)} \right]$. Since $\tilde{\delta}_t$ always decreases and its initial value is very small, $\tilde{\delta}_t^0 \propto \frac{J_\perp}{J_\parallel} \ll 1$, it is irrelevant.
- [8] P. Hasenfratz and F. Niedermayer, Phys. Lett. B **268**, 231 (1991)
- [9] D. Reznik *et al.*, Phys. Rev. B **54**, 14741 (1996); S. M. Hayden *et al.*, Phys. Rev. B **54**, 6905 (1996)
- [10] T. Matsuda and K. Hida, J. Phys. Soc. Jpn. **59**, 2223 (1990); K. Hida, *ibid* **59**, 2223 (1990); *ibid* **61**, 1013 (1992); A. W. Sandvik and D. J. Scalapino, Phys. Rev. Lett. **72**, 2777 (1994); A. V. Chubukov and D. K. Morr, Phys. Rev. B **52**, 3521 (1995).
- [11] S. Chakravarty and R. Orbach, Phys. Rev. Lett. **64**, 224 (1990).
- [12] T. Imai *et al.*, Phys. Rev. Lett. **70**, 1002 (1993).

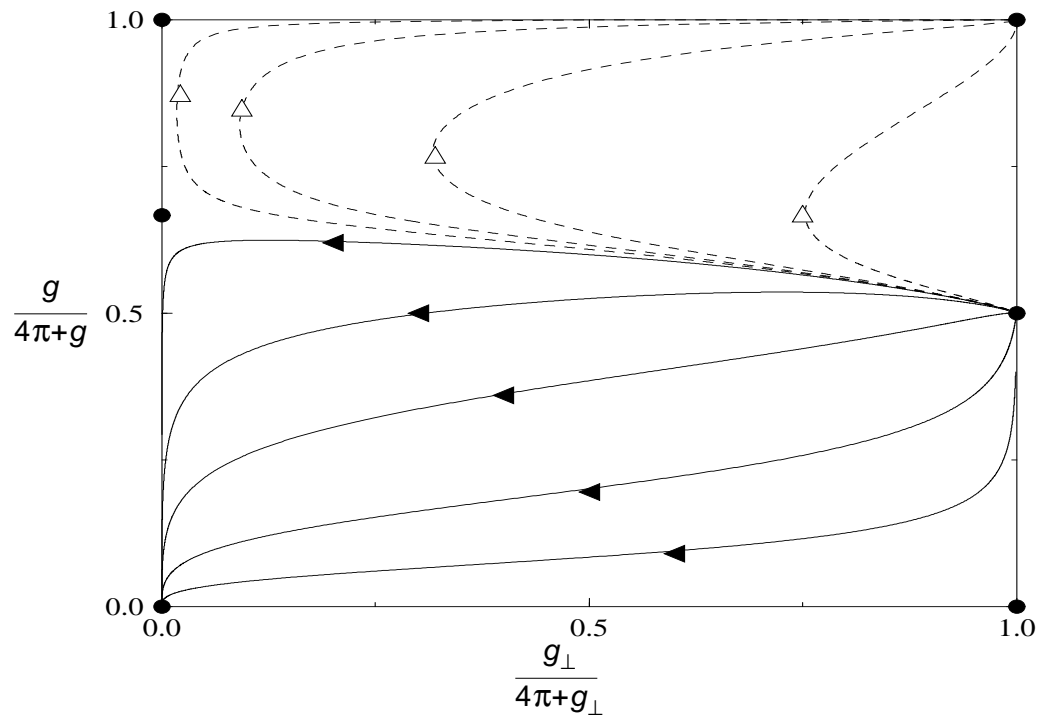


FIG. 1. Zero temperature flow diagram.